DELPHI Collaboration

DELPHI 2001-073 CONF 501
27 June, 2001

Search for a fermiophobic Higgs at LEP 2

Preliminary

S. Andringa[1], P. Gonçalves[1], A. Onofre[1], L. Peralta[1], M. Pimenta[1] and B. Tomé[1]

Abstract

Searches for a fermiophobic Higgs boson produced in association with a Z^0 boson and decaying to photon pairs are reported. All possible decays of the Z^0 bosons to fermions were considered, yielding $f\bar{f}\gamma\gamma$ final states. The analysed data were collected with the DELPHI detector since 1998 until the end of LEP, corresponding to centre-of-mass energies ranging from 189 GeV to 208 GeV, and to a total integrated luminosity of about 600 pb^{-1}. The data were found to be in agreement with the Standard Model predictions. 95% C.L. upper limits on the cross-section of the process $e^+e^- \to h^0Z^0$, with h^0 decaying to two photons, were derived as a function of the Higgs boson mass. This bound was translated to a 95% C.L. lower limit of 103.4 GeV/c^2 on the mass of a fermiophobic Higgs boson with Standard Model-like couplings to the gauge bosons but with no couplings to fermions.

Contributed Paper for EPS HEP 2001 (Budapest) and LP01 (Rome)

[1] LIP-IST-FCUL, Av. Elias Garcia, 14, 1, P-1000 Lisboa, Portugal

1 Introduction

The decay of the Higgs boson to photons within the Standard Model (SM) proceeds via loops of heavy charged particles, namely W bosons and top-quarks, and the corresponding branching ratio (BR) is below 0.1%. The experimental signature of a two-photon resonance is, on the other hand, clear enough to make this decay mode one of the main channels for Higgs searches at hadron colliders.

At LEP, this search is motivated by extensions of the SM. In fact, many of the purposed models may enhance this branching ratio, either by enlarging the $H\gamma\gamma$ coupling [1] or by reducing the coupling of the Higgs to fermions [2]. In any case, the Higgs boson can be produced in association with a Z^0 boson and thus the existence of a massive two photon resonance accompanied by a fermion pair can be a clear indication of New Physics.

We present updated analyses of final states with isolated photons using the data collected with the DELPHI detector at LEP corresponding to centre-of-mass energies ranging from 189 GeV and 208 GeV and to a total integrated luminosity of about 600 pb^{-1}. An analysis of $l^+l^-\gamma\gamma$ final states, corresponding to the Z^0 boson decays to lepton pairs, is included for the first time.

The production of h^0Z^0 with $h^0 \to \gamma\gamma$ has been investigated previously and interpreted in several frameworks: previous analyses of DELPHI data can be found in [3] and results from other LEP experiments are reported in [4]; combined LEP results are described in [5].

2 Data Samples

The data analysed were collected during the LEP runs of 1998, 1999 and 2000. The corresponding centre-of-mass energies ($\sqrt{s}$) and integrated luminosities ($\mathcal{L}$) are shown in table 1.

year	1998	1999				2000		
$\sqrt{s}$ (GeV)	189	192	196	200	202	205	206*	207
$\mathcal{L}$ (pb^{-1})	153	25	76	83	40	78	59	84

Table 1: Centre-of-mass energies and integrated luminosities of the analysed samples. The 206 GeV data sample was not used in the leptonic channel and only 54 pb^{-1} of these data were used in the missing energy channel.

In 2000, the centre-of-mass energies ranged from 200 GeV to 209 GeV. The data corresponding to the last 59 pb^{-1} collected with DELPHI, and to an average centre-of-mass energy of 206 GeV, were analysed separately. The reason for this procedure lay in a malfunction of one sector, corrresponding to 1/12 of the coverage, of the main DELPHI tracking device (the TPC). This problem, however, did not affect much the present analyses. The remaining data taken during the year 2000 were divided in two different sets, corresponding to data taken at centre-of-mass energies around 205 GeV and around 207 GeV.

Signal events corresponding to several different Higgs boson masses and to all Z^0 boson decays were generated using PYTHIA 6.1 [6]. The background process $e^+e^- \to Z^0/\gamma^* \to q\bar{q}(\gamma)$ was also generated with PYTHIA 6.1 [6]; $e^+e^- \to Z^0 \to l^+l^-(\gamma)$ ($l = \mu, \tau$) and $e^+e^- \to Z^0 \to \nu\bar{\nu}(\gamma)$ events were generated with KORALZ [7] ; $e^+e^- \to e^+e^-(\gamma)$

events were produced with BHWIDE[8]; Compton-like final states originating from an $e\gamma$ collision (with a missing electron in the beam pipe) were generated according to [9]; for 4-fermion processes, EXCALIBUR [10] and GRC4F [11] were used and the QED process $e^+e^- \to \gamma\gamma(\gamma)$ was produced according to [12]. The two-photon ("$\gamma\gamma$") physics events were generated according to the TWOGAM [13] generator for quark channels and the Berends, Daverveldt and Kleiss generator [14] for the electron, muon and tau channels. All the generated sets, at different centre-of-mass energies, were passed through the DELPHI simulation and reconstruction chain[15]. Dedicated samples were used to match the data affected by the TPC problem.

A detailed description of the DELPHI detector and its performance can be found in [15]. The most relevant subdetectors for the present analyses were the electromagnetic calorimeters: the High density Projection Chamber (HPC) in the barrel region, and the Forward ElectroMagnetic Calorimeter (FEMC) in the endcaps. The FEMC covers polar angles[1] between 11° and 35°. The HPC covers polar angles above 42° and consists of 144 modules, with azimuthal intermodular regions at $\mathrm{mod}(\phi, 15°) = 7.5°$, in which the detection of photons can be complemented by the use of the Hadronic CALorimeter (HCAL) information, which covers polar angles above 11°

The most relevant tracking devices were the Vertex Detector (VD), the Inner Detector (ID) and the Time Projection Chamber (TPC), covering polar angles above 20°. The tracking system in the barrel region is complemented by the information provided by the Outer Detector (OD) and in the endcaps by the Forward Chambers A and B (FCA, FCB).

The VD is crucial for the determination of secondary vertices and the tagging of b-quark jets and, most important for the present analysis, in the discrimination between photons converting inside the tracking system but after the VD and charged particles coming from the interaction point.

3 Event selection

The analysis of events with isolated photons was done in several steps. First a general selection was applied and isolated photons and leptons were reconstructed. To begin with, all events were required to contain at least one charged or neutral object with energy above 5 GeV in the polar angle region above 20°.

In the reconstruction of isolated particles, only good charged particle tracks were considered. Such classification corresponds to charged objects with momentum greater than 0.1 GeV/c and impact parameters below 4 cm in the transverse plane and below 4 cm /$\sin\theta$ in the beam direction. Energy deposits in the calorimeters unassociated to charged particle tracks were used in the reconstruction of isolated objects only if their energy was above 0.3 GeV.

The reconstruction of isolated particles consisted on constructing double cones centered around the direction of the charged particle tracks and of the neutral energy deposits. The energy inside an inner cone , with half opening angle of 5° (10° for the topology with only photons), was required to be above 4 GeV, while the energy contained between the inner cone and the outer cone was required to be small to ensure isolation. Both the opening angle of the outer cone and the cut on the energy contained between the two

[1]The polar angle (θ) is defined in relation to the beam axis. In all cases also the complementary value (180.-θ) is assumed.

cones were allowed to vary according to the topology of the event and to the energy and classification of the reconstructed particle.

Charged and neutral isolated particles yielding energy deposits in the HPC were considered photon or electron candidates if there was no HPC layer with more than 90% of their electromagnetic energy. Moreover, particles yielding hadronic energy deposits above 3 GeV were required to have deposited more than 90% of their hadronic energy in the first layer of the HCAL in order to be considered electron or photon candidates.

A VD track element was defined as at least two signals in different VD layers separated in azimuthal angle by at most 0.5°. Isolated particles (charged or neutral) were associated to VD track elements if their azimuthal direction coincided within 3° in the barrel (10° in the forward region) with the azimuthal direction of the VD track element. Isolated charged particles contained within the polar angle range of the VD were taken as isolated lepton candidates if there were associated to VD track elements. Alternatively, isolated charged particles not associated to VD track elements were considered candidates for converted photons. Isolated charged particles associated to signals in the muon chambers, and for which the ratio between the associated energy and the measured momentum was less than 20%, were identified as muons.

Only events with visible energy in the polar angle region above 20° greater than $0.2\sqrt{s}$ were accepted (except for the topology with only photons, where this threshold was lowered to $0.1\sqrt{s}$). This requirement vetoes most of the contamination from "$\gamma\gamma$" collisions. Only photons with more than 5 GeV were considered in the analyses. At most one converted photon candidate was allowed per event, except for the $l^+l^-\gamma\gamma$ topologies where no recovery of converted photons was performed.

3.1 Two photons and two jets

For the hadronic topologies it was required that at least six good charged particle tracks were present. All selected charged and neutral particles not associated to isolated photons or leptons were clustered into two jets using the DURHAM jet algorithm [16].

The main background for this search, indeed irreducible, is $q\bar{q}$ production with two photons coming mainly from initial state radiation (ISR): at LEP 2, in about half the $q\bar{q}$ events, the beam electrons (positrons) radiate highly energetic photons, lowering the effective collision energy ($\sqrt{s'}$) down to M_{Z^0}. Very small contributions from other sources, namely from W^+W^- production, are also present.

selection	data	bkg	$q\bar{q}$	eff_{50}	eff_{100}
2 photons	**338**	**338.7**	287.9	60%	60%
anti-ISR/FSR	**23**	**17.0**	15.9	39%	45%
E-P-M_{Z^0} fit	**12**	**8.26**	8.13	31%	41%
$E_{\gamma 1} - E_{\gamma 2}$	**9**	**5.90**	5.80	26%	40%
HPC	**9**	**5.64**	5.54	26%	40%

Table 2: Evolution of the total $q\bar{q}\gamma\gamma$ sample collected in the year 2000 with analysis cuts. The number of selected events in data is compared to the expected background (total and $q\bar{q}$ background). The efficiencies for Higgs masses of 50 GeV/c^2 and 100 GeV/c^2 are also shown.

Table 2 shows the evolution of the data sample collected in 2000, corresponding SM

background and efficiencies for two Higgs signals of different masses, with the cuts. The preselection level corresponded to requiring two identified photons in the event. Further requirements were imposed in the isolation and polar angle of isolated particles in order to reduce both the ISR and final state radiation (FSR) contributions. Namely, the contribution of events in which the photons came from FSR was reduced by requiring that the most energetic photon had at least 15% of the beam energy, and that the minimum transverse energy of the photons with respect to any jet was above 7.5 GeV. A wide contribution from events in which one or two photons came from ISR was eliminated requiring that the minimum polar angle of the photons was above 30°. With exception of the two photons, no other isolated particles with transverse energy with respect to any of the jets greater than 20 GeV were allowed in the event.

To improve the mass resolution of the photon pair, a kinematic fit imposing energy-momentum conservation and constraining the jet-jet invariant mass to be the Z^0 mass was performed according to [17]. If both photons were away from the boundaries of the calorimeters and the normalized χ^2 (χ^2/ndof) associated to the photons was below 5 the events were kept. The χ^2/ndof for the photons was evaluated from:

$$\left(\frac{\chi^2}{\mathrm{ndof}}\right)^{photons} = \frac{1}{2}\sum_{i=1,2}\left(\frac{E_{\gamma i}^{fit} - E_{\gamma i}^{meas}}{\sigma_{\gamma i}^{meas}}\right)^2 \quad (1)$$

where E_γ^{meas} and E_γ^{fit} are respectively the measured and fitted photon energies and $\sigma_{\gamma i}^{meas}$ is the uncertainty associated to E_γ^{meas}. For events in which one of the photons was at a calorimeter boundary, the total χ^2/ndof of the fit was required to be below 5. Events in which both photons were not well contained in the calorimeters were rejected. As an effect of the previous requirements, the non $q\bar{q}$ background became almost negligible.

The characteristics of the radiative return to the Z^0 were then used to further reduce the background. In most of the radiative return events the photons are emitted at low polar angle and, in the majority of such events, one of the photons carries most of the energy necessary to lower $\sqrt{s'}$ down to M_{Z^0}, $E_{ret} = \frac{s - M_Z^2}{2\sqrt{s}}$. Therefore, only events in which the difference between the energies of the two photons was lower than $0.7E_{ret}$ were kept. Figure 1 shows the sum of the energies of the two photons and the difference between them, normalized to the radiative return energy (E_{ret}), before the last requirement was imposed.

In the final sample, one of the photons was required to be inside the HPC. Figure 2 shows the distributions of the reconstructed jet-jet invariant masses and of the fitted $\gamma\gamma$ invariant masses for the events selected from all analysed data samples, compared both to the SM background expectations and a Higgs signal.

3.2 Two photons and missing energy

All purely photonic candidate events were allowed to have at most 5 good charged particle tracks, none of them associated to VD track elements or to signals in the muon chambers. Charged particle tracks not associated to energy deposits above 5 GeV had to have momenta below 5 GeV/c.

The two photons were required to have polar angles above 25° and to be well contained either in the FEMC or in the HPC ($\theta < 35°$ or $\theta > 43°$) and, if they were in the same hemisphere, the minimum transverse energy between them had to be above 5 GeV.

Cosmic-rays crossing the detector outside the tracking devices and leaving only energy deposits in the calorimeters, are an important source of background for final states with

photons and missing energy. Most cosmic-ray events crossing the tracking system are removed by requiring than the impact parameters of the charged particle tracks are below 4 cm in the transverse plane and below 4 cm/$sin\theta$ in the beam direction. The remaining cosmic-ray events were vetoed requiring that the visible energy in the polar angle region above 20° (below 160°) was below $1.5\sqrt{s}$, that the hadronic energy associated to each photon was less than 98% of its total energy and that for photons reconstructed in the HPC, the direction of the shower was consistent with the hypothesis that the particle was coming from the primary vertex within 10°.

The main background process for this channel is the production of $\nu\bar{\nu}$ pairs (either through Z^0 or $W^{\pm}$ boson exchange) along with the emission of ISR photons. This process has a low cross-section but is an irreducible source of background. The QED process $e^+e^- \to \gamma\gamma(\gamma)$ has a much higher cross-section and is also a source of background, which can however be dramatically reduced by the appropriate kinematic requirements. These requirements consisted of imposing that the angle between the two photons was less than 178° and that the acoplanarity between them was greater than 1° (3° if the direction of either one of the photons coincided with the HPC intermodular divisions). Moreover, only events in which the sum of the energies of the two photons was less than $0.65\sqrt{s}$ and in which the energy of the most energetic photon was less than 20% of the beam energy were accepted.

The missing mass of the remaining events was required to be larger than 20 GeV/c^2. A kinematic fit was then performed, imposing the Z^0 boson mass on the invisible system. The χ^2/ndof of the fit was required to be less than 10. Figure 3 shows the χ^2/ndof of the fit and the sum of the two photon energies normalized to $\sqrt{s}$ corresponding to all analysed data samples compared to the SM backgrounds and to a Higgs signal.

Table 3 shows the numbers of events at each selection level and corresponding background prediction for the data collected during the year 2000 along with the signal selection efficiencies for two Higgs masses. The reconstructed missing mass and the fitted $\gamma\gamma$ invariant mass are compared in figure 4 to the SM background and to a Higgs signal.

selection	data	bkg	QED	$\nu\bar{\nu}\gamma\gamma(\gamma)$	eff_{70}	eff_{110}
2 photons+cosmic veto	**1089**	**1132.0**	1121.0	11.0	64%	73 %
QED veto	**12**	**8.5**	1.1	7.4	51%	59 %
E-P-M_{Z^0} fit	**6**	**6.9**	0.8	6.1	48%	59 %

Table 3: Numbers of events selected in the data collected in year 2000 for each $\nu\bar{\nu}\gamma\gamma$ selection level, with corresponding background prediction and signal selection efficiencies for Higgs masses of 70 GeV/c^2 and 110 GeV/c^2 produced at a centre-of-mass energy of 206 GeV.

3.3 Two photons and two charged leptons

At the preselection level only events with at most five good charged particle tracks were kept. The presence of two isolated photons and two isolated leptons was required. The most energetic photon was required to have energy greater than $0.1\sqrt{s}$ and the polar angle of the leptons was required to be above 20° (except for leptons identified as muons).

The background processes for the present channels include $e^+e^- \to Z^0 \to l^+l^-(\gamma)$ and the t-channel Bhabha scattering, which has a very large cross-section. To reduce FSR events the minimum transverse energy of the photons with respect to the leptons was

required to be greater than 5 GeV. The contribution from double radiative return events was reduced requiring that both photons had polar angles above 30°, that there was at least one photon in the HPC and imposing that the difference between the energies of the two photons was below $0.7E_{ret}$.

A kinematic fit imposing energy-momentum conservation, and using the measured directions of the four particles in the event, was performed. Events were accepted only if the χ^2/ndof associated to the photons or the χ^2/ndof associated to the leptons was less than 10. Finally, the lepton pair was required to originate from a Z^0 decay by selecting only events with a di-lepton invariant mass (computed using the fitted energies and momenta) between 60 GeV/c^2 and 120 GeV/c^2. No lepton identification was performed.

Table 4 shows the numbers of events present in the real and simulated data sets, for the energies collected in the year 2000, at each selection level as well as signal detection efficiencies (flavour independent) for two different signal masses. In table 5, the signal detection efficiencies at the final selection level computed separately for each Z^0 boson decay mode are displayed together with the flavour independent efficiency used in the limits.

Figure 5 shows the fitted l^+l^- invariant mass distribution after the preselection and the fitted $\gamma\gamma$ invariant masses of the candidates compared to the SM prediction and to a signal.

selection	data	bkg	eff_{50}	eff_{100}
preselection	**17**	**21.9**	36%	36 %
anti-ISR/FSR	**4**	**4.3**	22%	31%
$E-P$ fit + M_{Z^0}	**0**	**1.3**	17%	27 %

Table 4: Numbers of events found in the data collected in 2000 for each selection level of the $l^+l^-\gamma\gamma$ analysis compared to the background prediction. Signal selection efficiencies are shown for Higgs of masses of 50 GeV/c^2 and 100 GeV/c^2 produced at a centre-of-mass energy of 200 GeV.

Z $\rightarrow$	e^+ e^-	$\mu^+\mu^-$	$\tau^+\tau^-$	l^+l^-
eff_{50}	20%	22%	9%	17%
eff_{100}	29%	38%	13%	27%

Table 5: $l^+l^-\gamma\gamma$ efficiencies for Higgs masses of 50 GeV/c^2 and 100 GeV/c^2 at $\sqrt{s}$ = 200 GeV, computed separately for each Z^0 decay mode. The global efficiency is shown in the last column.

4 Results

In table 6, the final numbers of events selected for all Z^0 decay modes and for all data samples are compared with the SM prediction. The Standard Model expectations were, in the case of final states with only photons, corrected for trigger efficiencies. A global agreement between data and MC expectations was found. The small excess found in

the $q\bar{q}\gamma\gamma$ channel, was present for most data samples, but was not concentrated in any particular $\gamma\gamma$ invariant mass region.

$\sqrt{s}$	$\mathcal{L}$	$q\bar{q}\gamma\gamma$		$\nu\bar{\nu}\gamma\gamma$		$l^+l^-\gamma\gamma$	
(GeV)	(pb^{-1})	DATA	MC	DATA	MC	DATA	MC
189	153	6	5.6 $\pm$0.7	6	5.3 $\pm$0.6	1	1.7 $\pm$0.4
192	25	0	0.9 $\pm$0.1	1	1.0 $\pm$0.1	0	0.3 $\pm$0.1
196	76	4	2.5 $\pm$0.4	2	2.4 $\pm$0.3	2	0.6 $\pm$0.1
200	83	4	2.4 $\pm$0.2	3	2.6 $\pm$0.3	0	0.6 $\pm$0.1
202	40	3	1.1 $\pm$0.1	0	1.1 $\pm$0.1	0	0.3 $\pm$0.1
205	78	3	1.9 $\pm$0.1	2	2.5 $\pm$0.3	0	0.6 $\pm$0.2
206	59	3	1.6 $\pm$0.1	4	1.8 $\pm$0.2	–	–
207	84	3	2.2 $\pm$0.1	0	2.6 $\pm$0.3	0	0.7 $\pm$0.2
total	598	26	18.2 $\pm$0.9	18	19.3 $\pm$0.9	3	4.7 $\pm$0.5

Table 6: Final numbers of events selected in all the analysed data sets for all topologies and corresponding number of expected SM background events (with statistical errors). For the $l^+l^-\gamma\gamma$ topologies, the data set corresponding to a centre-of-mass energy of 206 GeV was not included in the analysis.

Limits on the production cross-section of h^0Z^0 with $h^0 \to \gamma\gamma$ as a function of M_{h^0}, were obtained by combining all the data using the Modified Frequentist Likelihood Ratio method [18], taking into account the measured and expected mass distributions.

Figure 6 shows the 95% C.L. lower limits on the h^0Z^0 production cross-section multiplied by BR($h^0 \to \gamma\gamma$), normalized to the SM HZ^0 production cross-section, Taking 2HDM models [2] as a reference and for the range of Higgs masses considered, the width of the Higgs boson is always below the mass resolution of the analyses.

A 95% confidence level (C.L.) lower limit on M_{h^0} can be obtained at the intersection of the 95% C.L. cross-section upper limit with the branching ratio of $h^0 \to \gamma\gamma$ curve. Figure 6 shows also a fermiophobic BR curve, computed assuming that the Higgs couplings to bosons have SM values, but the couplings to fermions vanish, is shown. In this model, a 95% C.L. lower limit of 103.4 GeV/c^2, on the mass of such a Higgs boson is obtained while the expected limit was of 105.1 GeV/c^2.

5 Conclusions

Around 600 pb^{-1} of LEP2 data, corresponding to centre-of-mass energies between 189 GeV and 208 GeV, were analysed in the search for h^0Z^0 production with subsequent h^0 decay to two photons. All possible Z^0 boson decays were analysed. A fair agreement between the analysed data and the Standard Model expectations was found and a 95% C.L. upper limit on the h^0Z^0 production cross-section for M_{h^0} up to 115 GeV/c^2 was derived. A 95% C.L. lower limit of the mass of a fermiophobic Higgs boson (with vanishing couplings to fermions) of 103.4 GeV/c^2 was obtained, while the corresponding expected limit was of 105.1 GeV/c^2.

References

[1] K. Hagiwara, R. Szalapski and D. Zeppenfeld, Phys. Lett. **B318** (1993) 155;
K. Hagiwara, S. Ishihara, R. Szalapski and D. Zeppenfeld, Phys. Rev. **D48** (1993) 2182.

[2] A. Barroso, L. Brücher, R. Santos, Phys. Rev. **D60** (1999) 035005;
L. Brücher, R. Santos, Eur. Phys. J. **C12** (2000) 87.

[3] DELPHI Coll., P. Abreu et al., Phys. Lett. **B458** (1999) 431;
DELPHI Coll., P. Abreu et al., Phys. Lett. **B507** (2001) 89.

[4] ALEPH Coll.,R. Barate et al., Phys. Lett. **B487** (2000) 241;
L3 Coll., M.Acciarri et al., Phys. Lett. **B489** (2000) 115;
OPAL Coll.,G. Abbiendi et al., Phys. Lett. **B464** (1999) 311.

[5] ALEPH, DELPHI, L3 and OPAL Coll. and the LEP working group for Higgs boson searches, "Searches for Higgs bosons: Preliminary combined results using LEP data collected at energies up to 202 GeV", CERN-EP-2000-055.

[6] T. Sjöstrand, Comp. Phys. Comm. **82** (1994) 74;
T. Sjöstrand, Pythia 5.7 and Jetset 7.4, Cern-TH/7112-93.

[7] S. Jadach, B.F.L. Ward and Z. Wąs, Comp. Phys. Comm **66** (1991) 276.

[8] S. Jadach, W. Placzek and B.F.L. Ward, Phys. Lett. **B390** (1997) 298.

[9] D. Karlen, Nucl. Phys. **B289** (1987) 23.

[10] F.A. Berends, R. Pittau and R. Kleiss, Comp. Phys. Comm **85** (1995) 437.

[11] J.Fujimoto et al., Comp. Phys. Comm. **100** (1997) 128.

[12] F. Berends and R. Kleiss, Nucl. Phys. **B186** (1981) 22.

[13] S. Nova, A. Olchevski and T. Todorov, "TWOGAM, CERN report 96-01, vol.2 p. 224 (1996).

[14] F.A. Berends, P.H. Daverveldt and R. Kleiss, Comp. Phys. Comm. **40** (1986) 271.

[15] DELPHI Coll., P. Aarnio et al., Nucl. Instr. and Meth. **A303** (1991) 233;
DELPHI Coll., P. Abreu et al., Nucl. Instr. and Meth. **A378** (1996) 57.

[16] S. Catani et al., Phys. Lett. **B269** (1991) 432.

[17] DELPHI Coll., P. Abreu et al., Eur. Phys. J. **C2** (1998) 581.

[18] A.L. Read, "Modified Frequentist Analysis of Search Results (The CLs Method)" in "Workshop on Confidence Limits", ed. F. James, L. Lyons and Y.Perrin, CERN Report 2000-005 (2000) p.81.

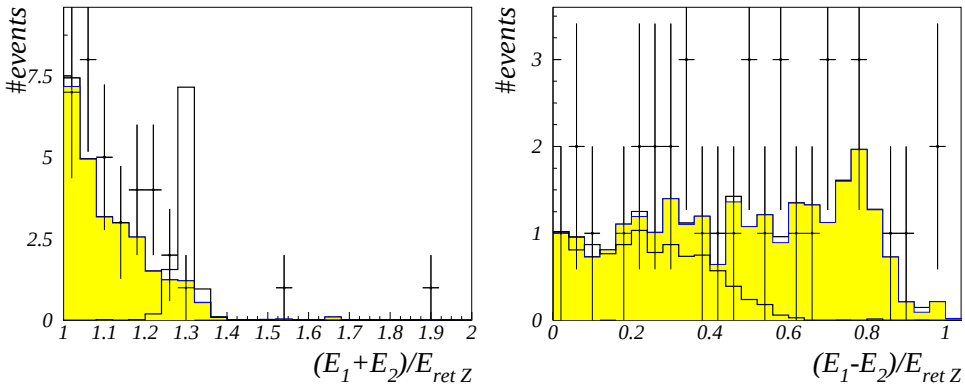

Figure 1: Sum (left) and difference (right) of the two photon energies in the $q\bar{q}\gamma\gamma$ final state normalized to the radiative return energy, for all data samples analysed. The data (dots) are compared with background expectations (shaded histogram). A signal for a 100 GeV/c^2 Higgs produced at 206 GeV with arbitrary cross-section is also shown as the tick line. The two events with high energy sum are removed by the cut on the energy difference.

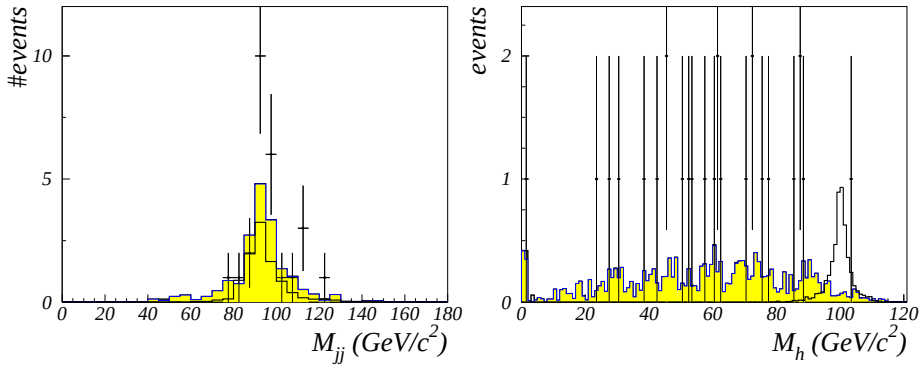

Figure 2: The jet-jet invariant mass reconstructed before any fit is shown on the left for all the $q\bar{q}\gamma\gamma$ events in the last selection level. On the right the fitted Higgs mass is shown. For both distributions the data (dots) are compared to the SM background prediction (shaded histogram). In addition to the data and background, a 100 GeV/c^2 Higgs signal produced at all energies with arbitrary cross-section, is also shown, as the thick line.

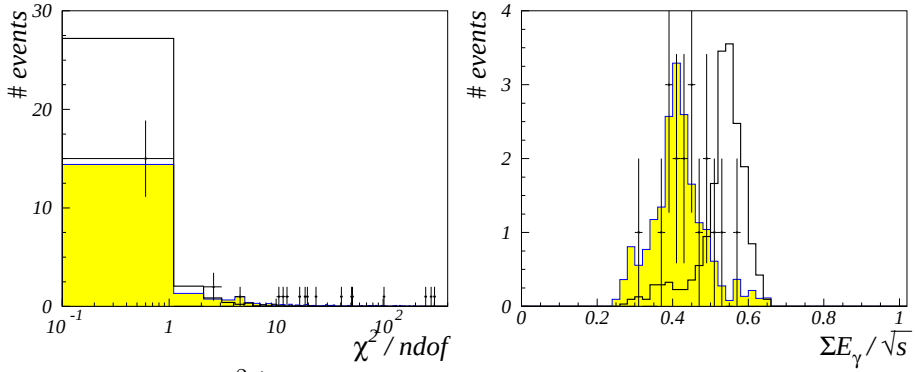

Figure 3: On the left, the $\chi^2/ndof$ of the fit imposing that the missing mass is compatible with the Z^0 mass is shown for data (dots) and SM processed (shaded histogram) for all the analysed data sets, in the two photons and missing energy channel. On the right, the sum of the energies of the two photons normalized to the centre-of-mass energy is compared to the SM prediction (shaded histogram) for the events with $\chi^2/ndof < 10$. A signal for a 110 GeV/c^2 Higgs boson produced at 206 GeV with arbitrary cross-section, is represented by the thick line.

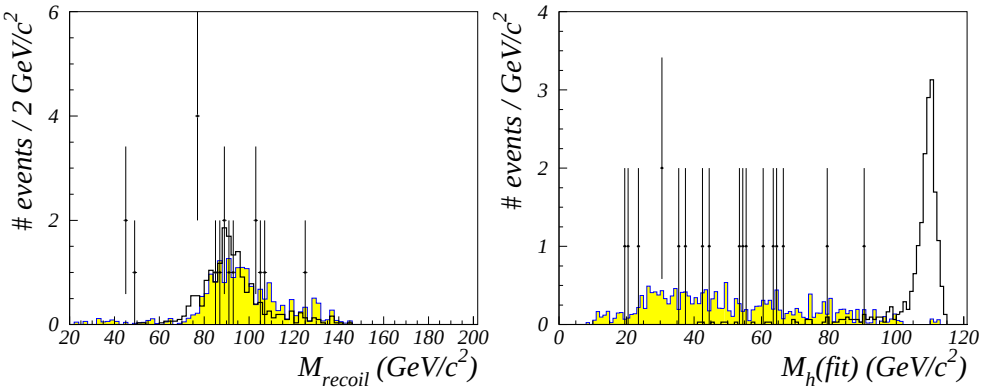

Figure 4: On the left, the measured missing mass is shown for all the $\gamma\gamma$ events present at the last selection level, the data (dots) are compared to the SM backgrounds (shaded histogram). On the right, the fitted Higgs boson mass obtained for the selected data events is compared to the respective SM expectations (shaded histogram). For both variables, the thick line represents a signal for a 110 GeV/c^2 Higgs boson produced at the centre-of-mass energy of 206 GeV, with arbitrary cross-section.

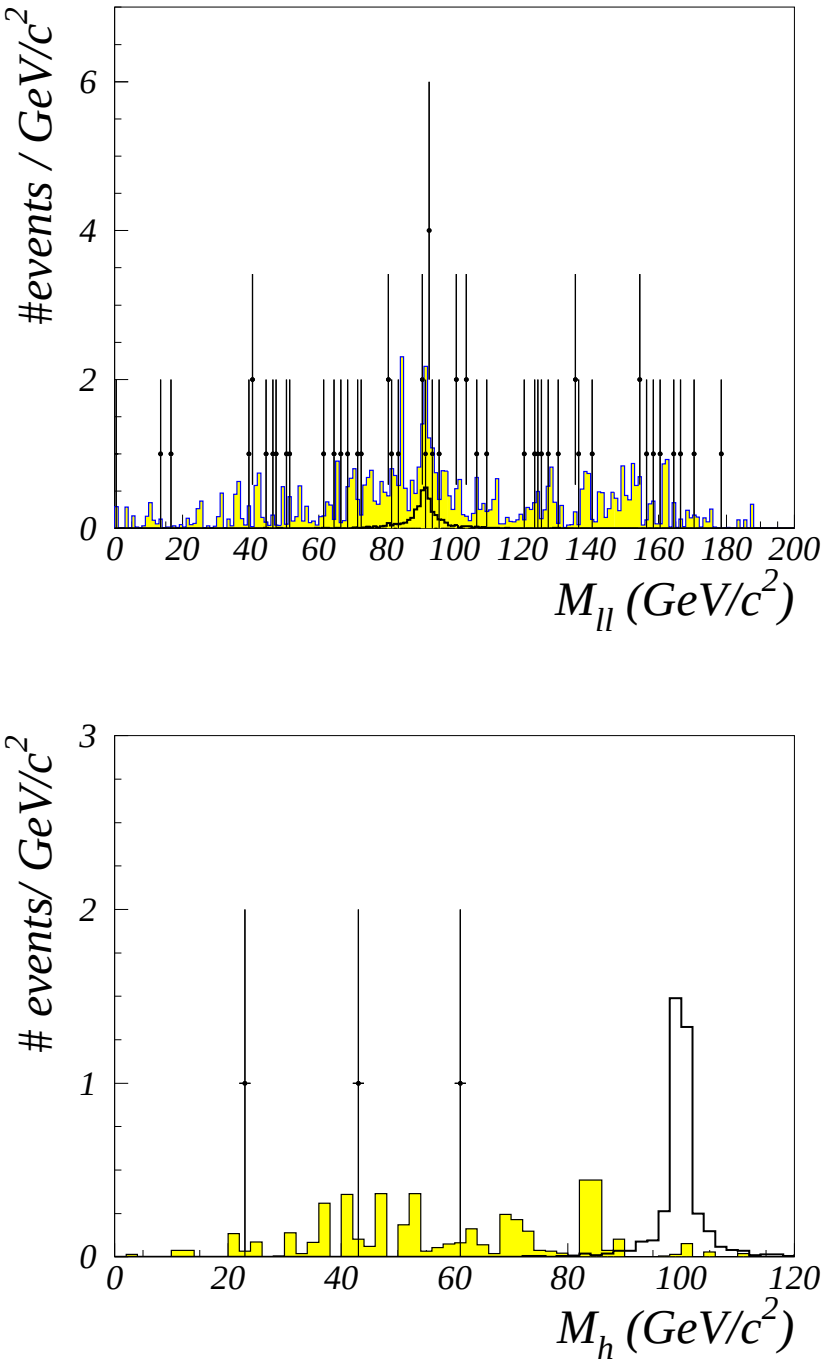

Figure 5: The top plot shows the fitted l^+l^- invariant mass at the preselection level for the data (dots) and the SM background (filled histogram); in the bottom plot the fitted Higgs boson mass distribution for the selected candidates is compared to the respective SM prediction. The expected distributions from a 100 GeV/c^2 Higgs signal (thick line) produced at $\sqrt{s}$ = 206 GeV, with arbitrary cross-section and including all $Z^0 \to l^+l^-$ decays are also displayed in both plots.

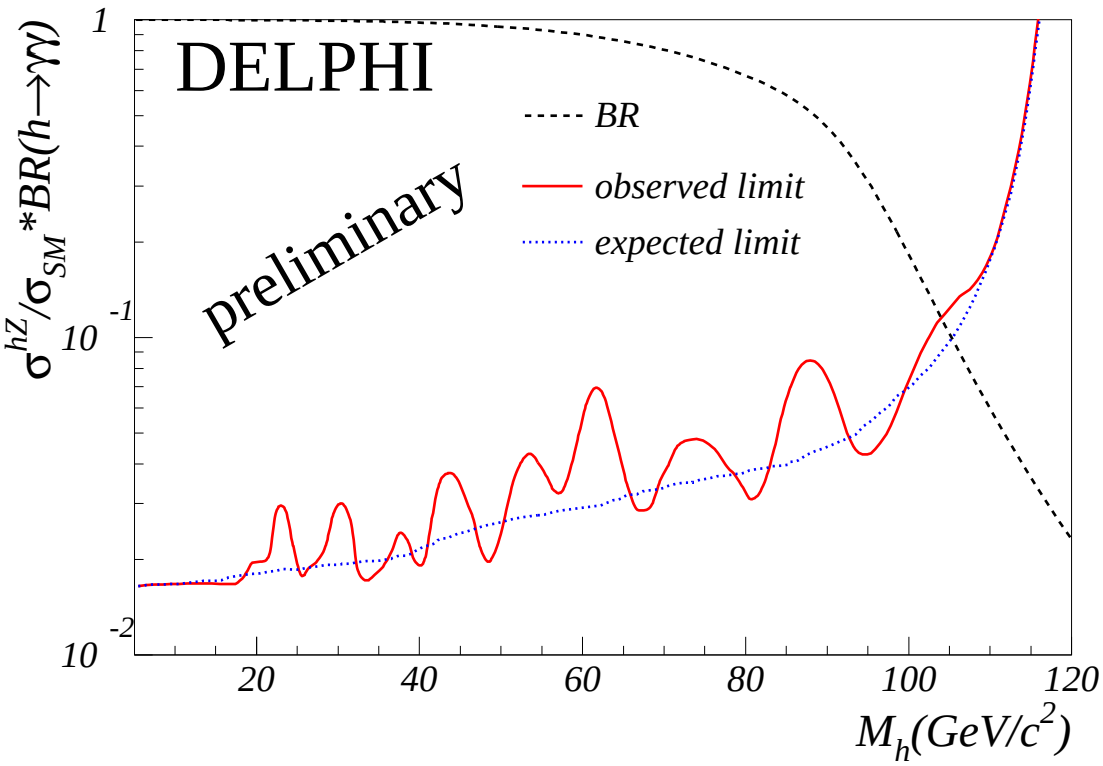

Figure 6: 95% C.L. observed (full line) and expected (dotted line) upper limits on the h^0Z^0 production cross-section normalized to the SM value (for the HZ^0 production cross-section) $\times$ BR($h^0 \to \gamma\gamma$). The fermiophobic branching ratio of $h^0 \to \gamma\gamma$ as a function of M_{h^0} is represented by the dashed line. The intersection of the observed (expected) limit on the cross-section with the BR curve yields a value of M_{h^0} of 103.4 GeV/c^2 (105.1 GeV/c^2) corresponding to the 95% lower limit in the mass of a fermiophobic Higgs boson.